

# Efficient Vision Transformer for Human Pose Estimation via Patch Selection

Kaleab A. Kinfu  
Johns Hopkins University  
kinfu@jhu.edu

René Vidal  
University of Pennsylvania  
vidalr@seas.upenn.edu

## Abstract

While Convolutional Neural Networks (CNNs) have been widely successful in 2D human pose estimation, Vision Transformers (ViTs) have emerged as a promising alternative to CNNs, boosting state-of-the-art performance. However, the quadratic computational complexity of ViTs has limited their applicability for processing high-resolution images and long videos. To address this challenge, we propose a simple method for reducing ViT’s computational complexity based on selecting and processing a small number of most informative patches while disregarding others. We leverage a lightweight pose estimation network to guide the patch selection process, ensuring that the selected patches contain the most important information. Our experimental results on three widely used 2D pose estimation benchmarks, namely COCO, MPII and OCHuman, demonstrate the effectiveness of our proposed methods in significantly improving speed and reducing computational complexity with a slight drop in performance.

## 1. Introduction

In recent years, Human Pose Estimation (HPE) has emerged as an important problem in computer vision, with numerous applications in fields such as surveillance [9], motion analysis [19], virtual and augmented reality [11, 13]. Classical algorithms relied on handcrafted features [5, 7, 15], but recent advances in deep learning have led to significant improvements [21, 26]. For instance, Convolutional Neural Networks (CNNs) have proven to be successful by exploiting spatial correlations among pixels.

The recent emergence of Vision Transformers (ViTs) has challenged the dominance of CNNs. Unlike CNNs, ViTs rely on self-attention mechanisms to model the long-range dependencies between patches, which has been shown to be highly effective [3]. Nevertheless, the computational complexity of ViTs presents a significant challenge for processing high-resolution images and long videos. The computational cost of ViTs scales quadratically as the number of input tokens increases, making them intractable for practical

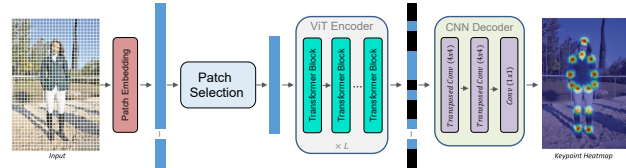


Figure 1. **Overall architecture of the proposed ViT-based HPE method with patch selection** – The input is fed to a patch embedding layer that divides the image into patches of size  $16 \times 16$ . Patch selection is performed before they are processed by ViT to reduce the computation. Then, a simple CNN decoder is fed with the featuremap generated by ViT, which includes zero-filled non-body-part patches, to generate the heatmap prediction.

use. To address this issue, several recent works have proposed various methods for reducing the number of tokens in ViTs, thereby lowering their computational cost.

Token Learner [18] is one approach that aims to identify and learn a small set of important tokens from the input. Token Pooling [12] clusters the tokens and down-samples them, whereas DynamicViT [16] introduces a token scoring network to identify and remove redundant tokens. Although these techniques successfully reduce the GFLOPs of ViTs in classification tasks, the additional pooling and scoring network can introduce additional computational overhead. Besides, the extension of these approaches to dense prediction tasks, such as HPE, remains an open question.

In this paper, we propose a standard Vision Transformer-based HPE with patch selection to greatly reduce computational complexity. Specifically, we propose two patch selection methods based on using lightweight pose estimation networks that are very fast but inaccurate. This leads to a significant reduction in computational complexity and improvements in speed with a slight drop in accuracy. To validate the effectiveness of our proposed approach, we conducted experiments on three common 2D pose estimation benchmarks: COCO, MPII, and OcuHuman. Our results demonstrate that our approach significantly reduces the computational cost while maintaining competitive accuracy compared to other state-of-the-art methods.

## 2. Related Work

### 2.1. Human Pose Estimation

Human pose estimation is a vital task in computer vision that involves identifying and estimating the location of human body parts from 2D images or videos. It has several applications, including human-computer interaction [8], action recognition [4, 24], virtual and augmented reality [11, 13], and surveillance [9]. In recent years, deep learning methods have been successful in 2D HPE, with most methods employing CNNs to learn a mapping between the input image and the corresponding 2D pose.

Single-person HPE is generally accomplished using two deep learning pipelines: regression-based or heatmap-based approaches, with the latter being the focus of this work. In the regression-based approach, the network learns a mapping from the input image to body keypoints via end-to-end training, treating the task as a joint position regression problem. The heatmap-based approach, on the other hand, predicts the approximate location of keypoints encoded via a 2D Gaussian heatmap centered at the body joint. Multi-person HPE is more challenging than single-person pose estimation, requiring the determination of the number of people, their positions, and how to group key points. Top-down and bottom-up approaches are used for multi-person pose estimation, with this work focusing on the former, which uses person detectors to extract a set of boxes from the input images and applies single-person pose estimators to each person box to produce multi-person poses.

### 2.2. Vision Transformer

The Vision Transformer (ViT) architecture proposed by Dosovitskiy *et al.* [3] has demonstrated remarkable performance on image classification tasks. However, it has quadratic computational complexity. To improve the efficiency of ViT, researchers have proposed methods such as sparsifying the attention matrix [2, 17], token pooling [12], and estimating the significance of tokens [16]. Hierarchical Visual Transformer [14] removes redundant tokens via token pooling, while TokenLearner [18] introduces a learnable tokenization module.

Specific to HPE, several transformer-based architectures have been proposed. Transpose [25] is a transformer network that estimates 2D pose using a CNN-based backbone and self-attention to model long-range dependencies. TokenPose [10] is another transformer based on explicit token representation for each body joint. HRFormer [27] is a transformer that adopts HRNet design along with convolution and local-window self-attention. ViTPose [23] is a ViT-based approach that uses Masked Auto Encoder (MAE) [6] pretraining and shared encoder training on multiple datasets to improve performance. These architectures demonstrate the effectiveness of transformer-based models in HPE.

## 3. ViT based Human Pose Estimation

In this section, we describe our approach to HPE, which includes revisiting the standard ViT-based method and incorporating a patch selection technique. We present the overall architecture of our method in Figure 1. Specifically, we use a ViT encoder as the model’s backbone and pass the encoder’s final featuremap to a CNN-based heatmap decoder, similar to the approach used in [23].

To begin, we embed an input image  $X \in R^{H \times W \times 3}$  into patches of size  $16 \times 16$ , resulting in a feature tensor  $F \in \mathbb{R}^{\frac{H}{16} \times \frac{W}{16} \times C}$ , where  $C$  represents the channel dimension. These embedded tokens are then processed by  $L$  transformer layers, each of which consists of a multi-head self-attention (MHSA) layer and a feed-forward network (FFN). The output of the ViT encoder is denoted as  $F_{out} \in \mathbb{R}^{\frac{H}{16} \times \frac{W}{16} \times C}$ , where  $F_{out}$  represents the final feature map produced by the ViT. Next, we use a classical decoder with two deconvolution blocks, each with a deconvolution layer, batch normalization, and ReLU activation.

### 3.1. Improving Efficiency via Patch Selection

Although ViT can model long-range dependencies and is able to generate a global representation of the overall image, the computational complexity increases quadratically. However, not all patches in an image contribute equally to the HPE task. Recent research [25] indicates that the long-range dependencies between predicted keypoints are mostly restricted to the body part regions. Therefore, computing MSA between every patch in the image while only a few patches are relevant to the body parts is unnecessary.

To this end, we propose two methods that use an off-the-shelf lightweight pose estimator to guide the selection of small relevant body part patches while discarding irrelevant and background patches without re-training the vision transformer. By selecting only the relevant patches, we can significantly reduce the computational complexity of ViT-based HPE, resulting in accurate yet efficient pose estimation. In this work, we present two approaches for selecting body-part relevant patches from a given pose estimation prediction  $\mathcal{B} \in \mathbb{R}^{K \times 2}$ , where  $K$  is the number of keypoints. Our first approach utilizes a breadth-first neighboring search algorithm, as outlined in Section 3.1.1. In our second approach, we select patches formed by a skeleton of the joints. Here, the objective is to select body patches where the lines formed by body joint pairs cross. To accomplish this, we utilize Bresenham’s algorithm to select the relevant patches, as outlined in Section 3.1.2. It is important to note, however, that by selecting a few patches of the image and processing it with the ViT encoder, we only get the features of the patches that were chosen. However, we must create a featuremap for all patches for further processing. As a result, since the goal of the HPE task is to produce a Gaussian heatmap centered at the body joint and

---

**Algorithm 1 (Select body part patches and neighbors given keypoint prediction)**


---

**Require:** keypoint prediction  $\mathcal{B} \in \mathbb{R}^{K \times 2}$ , patch size  $P$ , neighboring search function  $\mathcal{N}$  and  $n$  number of neighboring patches.

```

1: function SELECTJOINTPATCHES
2:    $BP = \{\}$   $\triangleright$  initialize the set of body part patches
3:   for  $k \leftarrow 1$  to  $K$  do  $\triangleright$  number of joints
4:      $x^k = \lfloor \frac{\mathcal{B}_x^k}{P} \rfloor, y^k = \lfloor \frac{\mathcal{B}_y^k}{P} \rfloor$   $\triangleright$  get column, row
5:     for  $(i, j) \in \mathcal{N}(x^k, y^k, n)$  do
6:        $p = (y^k + j) \times \frac{W}{P} + (x^k + i)$   $\triangleright$  1-D index
7:        $BP \leftarrow p$   $\triangleright$  add patch to the set
8:     end for
9:   end for
10: end function

```

---

zero elsewhere, we fill the non-body-part patches with zeros (see Figure 1).

---

**Algorithm 2 (Select body part patches formed by a skeleton given keypoint prediction)**


---

**Require:** keypoint prediction  $\mathcal{B} \in \mathbb{R}^{K \times 2}$ , body part pairs  $\mathcal{P}$ , patch size  $P$ ,  $n$  number of neighboring patches.

```

1: function SELECTSKELETONPATCHES
2:    $BP = \{\}$   $\triangleright$  initialize the set of body part patches
3:   for  $k \leftarrow 1$  to  $K$  do  $\triangleright$  number of joints
4:      $x_0^k = \lfloor \frac{\mathcal{B}_x^k}{P} \rfloor, y_0^k = \lfloor \frac{\mathcal{B}_y^k}{P} \rfloor$   $\triangleright$  get column, row
5:     for  $l \in \mathcal{P}(k)$  do  $\triangleright$  get joint pair
6:        $x_1^k = \lfloor \frac{\mathcal{B}_x^l}{P} \rfloor, y_1^k = \lfloor \frac{\mathcal{B}_y^l}{P} \rfloor$ 
7:        $\Delta_x = x_1 - x_0, \Delta_y = y_1 - y_0$ 
8:        $\epsilon = 2\Delta_y - \Delta_x$   $\triangleright$  init error
9:        $y = y_0$ 
10:      for  $x \in [x_0, x_1]$  do
11:         $BP \leftarrow (x, y)$   $\triangleright$  add patch to the set
12:        if  $\epsilon \geq 0$  then
13:           $y = y + 1$ 
14:           $\epsilon = \epsilon - 2\Delta_x$ 
15:        end if
16:         $\epsilon = \epsilon + 2\Delta_y$ 
17:      end for
18:    end for
19:  end for
20: end function

```

---

### 3.1.1 Neighboring patch selection method

In our first approach, we are provided with a prediction  $\mathcal{B} \in \mathbb{R}^{K \times 2}$  of human pose estimation via a lightweight pose estimation network, where  $K$  denotes the number of keypoints. To select the body part patch and its  $n$  neigh-

boring patches, we employ a Breadth-First Search (BFS) algorithm, as presented in Algorithm 1. Specifically, for every keypoint located at 2D patch location  $(x, y) \in \mathcal{B}$ , we identify the nearest four neighboring patches located at  $(x, y + 1)$ ,  $(x, y - 1)$ ,  $(x - 1, y)$ , and  $(x + 1, y)$ , and store them in a queue. We continue searching for neighboring patches until we have selected  $n$  patches, ensuring that we do not revisit any previously visited patches. To provide a visual representation of this approach, we depict in Figure 2 a skeletonized human figure where the red patches represent the keypoint patches and the set of orange patches correspond to the selected neighboring patches.

### 3.1.2 Skeleton patch selection method

A limitation of the aforementioned neighboring selection method is that it only covers the body joint patch and its neighbors. However, in our second approach, we aim to extend this method to encompass all patches between joints. Extending the neighboring selection method to cover all patches between joints can lead to improved performance in our pose estimation system. To achieve this, we adopt a different strategy by identifying the patches where the line formed by the body joint pair crosses, based on Bresenham’s algorithm [1].

Originally proposed as a canonical line-drawing algorithm for pixelated grids, our extension of Bresenham determines the patches that need to be selected in the line between  $(x_0, y_0)$  and  $(x_1, y_1)$ , corresponding to the start and end 2D locations of patches containing body joints. As we move across the  $x$ - or  $y$ - axis in unit intervals, we select the  $x$  or  $y$  value between the current and next value that is closer to the line formed by the body joint pairs. To make this decision, we require a parameter  $\epsilon$ . Our objective is to track the slope error from the last increment, and if the er-

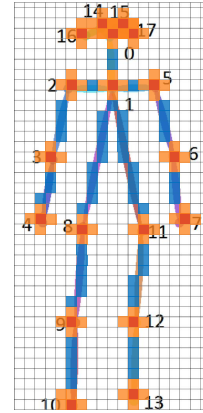


Figure 2. **Selected patches via the patch selection methods.** The red, orange, and blue patches correspond to the body keypoints, neighboring patches, and skeleton patches, respectively.

Table 1. Performance of the proposed patch selection methods ( $n = 7$ ) on three benchmarks, namely COCO, MPII, and OCHuman.

Model	Patch Selection	Input Resolution	Params	FLOPs	COCO Val AP	MPII PCKh	OCHuman AP
Lite-HRNet [26]	None	256 × 192	1M	0.2G	64.8	86.1	51.9
SimpleBaseline [22]	None	256 × 192	69M	15.7G	72.0	89.0	58.2
HRNet-W48 [20]	None	256 × 192	64M	14.6G	75.1	90.1	60.4
HRFormer-B [27]	None	256 × 192	43M	12.2G	75.6	-	49.7
ViTransPose-B	None	256 × 192	90M	17.9G	76.9	92.2	88.2
ViTransPose-B	Neighbors	256 × 192	90M	11.1G	73.4	91.5	84.7
ViTransPose-B	Skeleton	256 × 192	90M	13.3G	74.3	91.9	85.3
ViTransPose-L	None	256 × 192	309M	59.8G	78.7	92.8	91.5
ViTransPose-L	Neighbors	256 × 192	309M	35.6G	75.7	92.1	87.2
ViTransPose-L	Skeleton	256 × 192	309M	38.3G	76.3	92.4	89.8

ror exceeds a certain threshold, we increment our coordinate values and subtract from the error to re-adjust it to represent the distance from the top of the new patch, as presented in Algorithm 2. As depicted in Figure 2, the set of blue patches represents the patches selected by this approach.

## 4. Experiments

### 4.1. Implementation details

In our experiments, we employ the common top-down setting for human pose estimation. We follow most of the default training and evaluation settings of the mmpose framework but use the AdamW optimizer with a learning rate of  $5e - 4$  and UDP as a post-processing method. We use ViT-B and ViT-L as backbones and refer to the corresponding models as ViTransPose-B and ViTransPose-L. The backbones are pre-trained with MAE [6] weights.

### 4.2. Dataset details

The proposed methods for 2D pose estimation are evaluated on three benchmarks: COCO, MPII, and OCHuman. COCO, AI Challenger, and MPII are used to train the models, while OCHuman is used to test their performance in dealing with occlusion. The datasets are challenging and

diverse, with varying numbers of images, person instances, and annotated keypoints.

### 4.3. Evaluation metrics

The PCKh metric is used to evaluate performance on the MPII benchmark, while average precision (AP) is used on other benchmarks. AP is calculated using Object Keypoint Similarity (OKS), which measures how close predicted keypoints are to the ground truth keypoints.

### 4.4. Results

The performance of our proposed methods and other convolutional and transformer-based methods on three datasets, namely the COCO val set, the MPII test set, and the OCHuman test set, is presented in Table 1. Our experiments show that ViTransPose outperforms all, but is computationally expensive. However, our proposed patch selection method proves to be beneficial in this regard, as it significantly reduces computational costs while maintaining high accuracy. We used LiteHRNet [26], a lightweight and less accurate pose estimation network, to guide the patch selection method, which allowed us to achieve a significant improvement in efficiency with only a minor decrease in accuracy. We can also control the drop in accuracy by changing the number of neighboring patches. The trade-off between performance and computational complexity for the neighboring patch selection method is depicted in Figure 3.

## 5. Conclusion

In this work, we have proposed a method for reducing the computational complexity of Vision Transformers for human pose estimation. Our method tackles the challenge by selecting informative body part patches while discarding uninformative patches. The patch selection is guided by a lightweight pose estimation network. Our experimental results demonstrate that our methods are effective across three human pose estimation benchmarks.

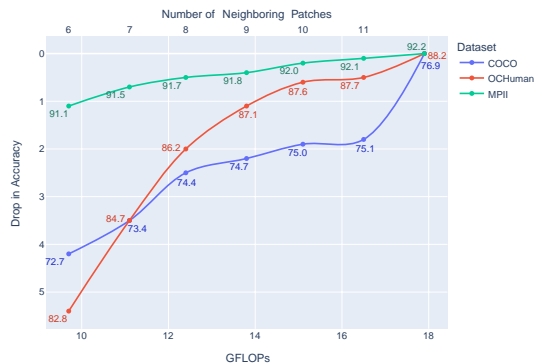


Figure 3. Trade-off between accuracy and GFLOPs of the neighboring patch selection method for the three benchmarks.

## References

- [1] Jack Bresenham. Algorithm for computer control of a digital plotter. *Seminal graphics*, 1965.
- [2] Rewon Child, Scott Gray, Alec Radford, and Ilya Sutskever. Generating long sequences with sparse transformers. *ArXiv*, abs/1904.10509, 2019.
- [3] Alexey Dosovitskiy, Lucas Beyer, Alexander Kolesnikov, Dirk Weissenborn, Xiaohua Zhai, Thomas Unterthiner, Mostafa Dehghani, Matthias Minderer, Georg Heigold, Sylvain Gelly, Jakob Uszkoreit, and Neil Houlsby. An image is worth 16x16 words: Transformers for image recognition at scale. *ArXiv*, abs/2010.11929, 2021.
- [4] Yong Du, Wei Wang, and Liang Wang. Hierarchical recurrent neural network for skeleton based action recognition. *2015 IEEE Conference on Computer Vision and Pattern Recognition (CVPR)*, pages 1110–1118, 2015.
- [5] Georgia Gkioxari, Pablo Arbeláez, Lubomir D. Bourdev, and Jitendra Malik. Articulated pose estimation using discriminative armllet classifiers. In *IEEE Conference on Computer Vision and Pattern Recognition*, pages 3342–3349, 2013.
- [6] Kaiming He, Xinlei Chen, Saining Xie, Yanghao Li, Piotr Dollár, and Ross B. Girshick. Masked autoencoders are scalable vision learners. *2022 IEEE/CVF Conference on Computer Vision and Pattern Recognition (CVPR)*, pages 15979–15988, 2022.
- [7] Sam Johnson and Mark Everingham. Clustered pose and nonlinear appearance models for human pose estimation. In *British Machine Vision Conference*, 2010.
- [8] Qiuhong Ke, Jun Liu, Bennamoun, Senjian An, Ferdous Sohel, and Farid Boussaid. Computer vision for human-machine interaction. 2018.
- [9] Alberto Lamas, Siham Tabik, Antonio Cano Montes, Francisco Pérez-Hernández, Jorge García-Torres Fernández, Roberto Olmos, and Francisco Herrera. Human pose estimation for mitigating false negatives in weapon detection in video-surveillance. *Neurocomputing*, 489:488–503, 2022.
- [10] Yanjie Li, Shoukui Zhang, Zhicheng Wang, Sen Yang, Wankou Yang, Shutao Xia, and Erjin Zhou. Tokenpose: Learning keypoint tokens for human pose estimation. *2021 IEEE/CVF International Conference on Computer Vision (ICCV)*, pages 11293–11302, 2021.
- [11] H. Lin and Ting-Wen Chen. Augmented reality with human body interaction based on monocular 3d pose estimation. In *ACIVS*, 2010.
- [12] Dmitrii Marin, Jen-Hao Rick Chang, Anurag Ranjan, Anish K. Prabh, Mohammad Rastegari, and Oncel Tuzel. Token pooling in vision transformers. *ArXiv*, abs/2110.03860, 2021.
- [13] Stepán Obdržálek, Gregorij Kurillo, Jay J. Han, Richard Ted Abresch, and Ruzena Bajcsy. Real-time human pose detection and tracking for tele-rehabilitation in virtual reality. *Studies in health technology and informatics*, 173:320–4, 2012.
- [14] Zizheng Pan, Bohan Zhuang, Jing Liu, Haoyu He, and Jianfei Cai. Scalable vision transformers with hierarchical pooling. *2021 IEEE/CVF International Conference on Computer Vision (ICCV)*, pages 367–376, 2021.
- [15] Deva Ramanan. Learning to parse images of articulated bodies. In *Neural Information Processing Systems*, 2006.
- [16] Yongming Rao, Wenliang Zhao, Benlin Liu, Jiwen Lu, Jie Zhou, and Cho-Jui Hsieh. Dynamicvit: Efficient vision transformers with dynamic token sparsification. In *NeurIPS*, 2021.
- [17] Aurko Roy, Mohammad Taghi Saffar, Ashish Vaswani, and David Grangier. Efficient content-based sparse attention with routing transformers. *Transactions of the Association for Computational Linguistics*, 9:53–68, 2021.
- [18] Michael S. Ryoo, A. J. Piergiovanni, Anurag Arnab, Mostafa Dehghani, and Anelia Angelova. Tokenlearner: What can 8 learned tokens do for images and videos? *ArXiv*, abs/2106.11297, 2021.
- [19] Jan Stenum, Cristina Rossi, and Ryan T. Roemmich. Two-dimensional video-based analysis of human gait using pose estimation. *PLoS Computational Biology*, 17, 2020.
- [20] Ke Sun, Bin Xiao, Dong Liu, and Jingdong Wang. Deep high-resolution representation learning for human pose estimation. *2019 IEEE/CVF Conference on Computer Vision and Pattern Recognition (CVPR)*, pages 5686–5696, 2019.
- [21] Alexander Toshev and Christian Szegedy. Deeppose: Human pose estimation via deep neural networks. *2014 IEEE Conference on Computer Vision and Pattern Recognition*, pages 1653–1660, 2014.
- [22] Bin Xiao, Haiping Wu, and Yichen Wei. Simple baselines for human pose estimation and tracking. In *ECCV*, 2018.
- [23] Yufei Xu, Jing Zhang, Qiming Zhang, and Dacheng Tao. Vit-pose: Simple vision transformer baselines for human pose estimation. *ArXiv*, abs/2204.12484, 2022.
- [24] Sijie Yan, Yuanjun Xiong, and Dahua Lin. Spatial temporal graph convolutional networks for skeleton-based action recognition. In *AAAI*, 2018.
- [25] Sen Yang, Zhibin Quan, Mu Nie, and Wankou Yang. Transpose: Keypoint localization via transformer. *2021 IEEE/CVF International Conference on Computer Vision (ICCV)*, pages 11782–11792, 2021.
- [26] Changqian Yu, Bin Xiao, Changxin Gao, Lu Yuan, Lei Zhang, Nong Sang, and Jingdong Wang. Lite-hrnet: A lightweight high-resolution network. *2021 IEEE/CVF Conference on Computer Vision and Pattern Recognition (CVPR)*, pages 10435–10445, 2021.
- [27] Yuhui Yuan, Rao Fu, Lang Huang, Weihong Lin, Chao Zhang, Xilin Chen, and Jingdong Wang. Hrformer: High-resolution transformer for dense prediction. *ArXiv*, abs/2110.09408, 2021.